Inorganic Chemistry

Article

pubs.acs.org/IC

Synthesis and Magnetic Properties of a New Borophosphate $SrCo_2BPO_7$ with a Four-Column Ribbon Structure

Wenbin Gou,[†,‡] Zhangzhen He,*[,†] Ming Yang,[†] Weilong Zhang,[†] and Wendan Cheng[†]

[†]State Key Laboratory of Structural Chemistry, Fujian Institute of Research on the Structure of Matter, Chinese Academy of Sciences, Fuzhou, Fujian 350002, China

[‡]Graduate University of the Chinese Academy of Sciences, Beijing 100039, China

Supporting Information

ABSTRACT: A new borophosphate $SrCo_2BPO_7$ is synthesized by a conventional high-temperature solid-state reaction. The titled compound is found to crystallize in monoclinic system with space group $P2_1/c$, which displays a distorted four-column ribbon structure. Both BO_3 triangles and PO_4 tetrahedra are isolated, while irregular triangles built by Co^{2+} ions are found to exist between the connecting ribbons. Magnetic behaviors are investigated by means of susceptibility, magnetization, and heat capacity measurements. The results confirm that $SrCo_2BPO_7$ possesses a three-dimensional antiferromagnetic ordering at 25 K. The possible spin arrangements in the system are also suggested.

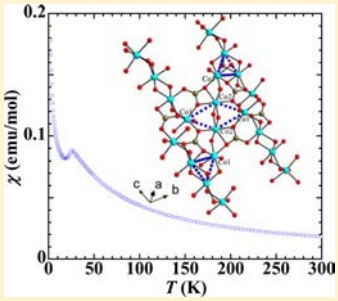

INTRODUCTION

Transition metal based phosphate compounds are potential materials for practical applications such as corrosion inhibition,[1] heterogeneous catalysis,[2] and ionic conductivity.[3] These materials provide rich structural chemistry since phosphate group serve as links for transition-metal polyhedra units giving rise to a variety of frameworks. Recently, compounds with a general formula of $AM_2(PO_4)_2$ (A = Ba, Sr, Pb; M = Cu, Ni, Co, Fe) have attracted much attention in solid state chemistry and physics, due to the discovery of their various interesting magnetic behaviors.[4−11] For example, $BaCu_2(PO_4)_2$ is a quasi-one-dimensional zigzag chain system with a spin singlet ground state,[4] while both $SrCu_2(PO_4)_2$ and $PbCu_2(PO_4)_2$ are spin-gap systems with a realization of a linear four-spin cluster model.[5,6] $BaNi_2(PO_4)_2$ exhibits a honeycomb spin-lattice which is likely a prototype of two-dimensional (2D) *XY* model,[7] while $SrNi_2(PO_4)_2$ is a three-dimensional (3D) antiferromagnet with two magnetic orderings at low-temperature.[8] $BaCo_2(PO_4)_2$ shows a $^1/_3$ plateau in the magnetization curve,[9] while $SrCo_2(PO_4)_2$ is a structurally four-spin system with an antiferromagnetic ordering at low temperature.[10] $SrFe_2(PO_4)_2$ is found to be a canted antiferromagnet with metamagnetic phase transition.[11]

On the other hand, borate compounds have also been a very active field of research for crystal chemistry, primarily due to the myriad of structural types arising from boron's triangular and tetrahedral coordination.[12] Current interest is focused on the main group metal borate compounds for their nonlinear optical applications.[13] However, transition metal borate compounds, warwickites formulated as $M^{2+}M^{3+}OBO_3$, are found to exhibit quite interesting magnetic behaviors.[14−19] For example, Fe_2OBO_3 and Mn_2OBO_3 are found to exhibit an unusual three-dimensional antiferromagnetic ordering that present a short-range ferromagnetic transition at low temperature,[15−17] while $MgVOBO_3$, $MgCrOBO_3$, and $MgTiOBO_3$ are identified to show spin glass behavior.[19] These compounds have a similar crystal structure, in which the same or different metal ions, M^{2+} and M^{3+}, are octahedrally coordinated by oxygen atoms and the octahedra are linked together by edge-sharing to form four-column ribbons, while boron atoms are associated with oxygen atoms to form planar triangular groups $(BO_3)^{3-}$ located in the voids between the ribbons.

A detailed structural comparison between phosphate and borate compounds has indicated that the PO_4 tetrahedra may be substituted by the BO_3 triangles for many phosphate compounds in some cases.[20] To explore new transition metal based oxides and to further investigate interesting magnetic phenomena, our current motivation is focused on borophosphate compounds through a partial substitution of BO_3 for PO_4 in phosphate compounds. In fact, only a few transition metal based anhydrous borophosphate compounds containing $M_2BP_3O_{12}$ (M = Fe, Cr, V),[21,22] Co_3BPO_7,[23] $Co_5BP_3O_{14}$,[24] and $BiM_2BP_2O_{10}$ (M = Co, Ni)[25] have been reported so far. In this work, a new borophosphate compound $SrCo_2BPO_7$ with a four-column ribbon structure is successfully obtained through the investigation of $SrO-CoO-B_2O_3-P_2O_5$ systems. Herein, we first report on synthesis, structure, and magnetic properties of $SrCo_2BPO_7$.

EXPERIMENTAL SECTION

Synthesis of $SrCo_2BPO_7$. Single crystals of $SrCo_2BPO_7$ were obtained by a standard solid-state reaction method using a mixture of high purity reagents of $SrCl_2·6H_2O$ (3N, 0.6968 g), $CoC_2O_4·4H_2O$

Received: November 2, 2012
Published: February 13, 2013

   dx.doi.org/10.1021/ic3023979 | *Inorg. Chem.* 2013, 52, 2492−2496

(3N, 1.0880 g), H_3BO_3 (3N, 0.2314 g), and $NH_4H_2PO_4$ (3N, 0.2875 g) as the starting materials. The mixture was ground carefully, homogenized thoroughly in an agate mortar, and then packed into an alumina crucible. The crucible was capped with a cover and then was put into the furnace. The furnace was heated up to 1050 °C and kept at 1050 °C for three days to ensure that the solution melts completely and homogeneously. The furnace was slowly cooled to 600 °C at a rate of 5 °C/h and then cooled to room temperature at a rate of 50 °C/h. With this procedure, red $SrCo_2BPO_7$ crystals were obtained by mechanical separation from the crucible. Powdered samples were synthesized by a high-temperature solid state reaction using a mixture of $SrCO_3$, $CoC_2O_4{\cdot}4H_2O$, H_3BO_3, and $NH_4H_2PO_4$ in a molar ratio of 1:2:1:1 at 900 °C for two days. The quality of samples was confirmed by powder X-ray diffraction (XRD), and the Rietveld refinement was also carried out. The results show that the observed XRD pattern agrees closely with the calculated pattern. The reliability factors were R_{wp} = 0.2961, R_p = 0.1830, and S = 2.010. The XRD data was indexed to the space group $P2_1/c$ with unit-cell parameters a = 6.485(3) Å, b = 9.270(9) Å, c = 10.066(5) Å, and β = 111.14(8)°. These parameters agree closely with ones obtained from a single crystal of $SrCo_2BPO_7$. No impurity phase was confirmed as seen in the Supporting Information (Figure S1).

X-ray Crystallography. Single crystals of $SrCo_2BPO_7$ were selected and mounted on glassy fibers for X-ray diffraction (XRD) measurements. Data collections of single crystals were performed at room-temperature on a Rigaku mercury CCD diffractometer equipped with a graphite monochromated Mo Kα radiation (λ = 0.710 73 Å). The structure was solved by direct methods and refined on F^2 by a full-matrix least-squares method using the SHELXL/PC programs.[26] The final refined structural parameters were checked by the PLATON program.[27] The crystal data and structure refinement information are given in Table 1. The final refined atomic positions and structural parameters are seen in the Supporting Information (Table S1–3).

Table 1. Crystal Data and Structure Refinement for $SrCo_2BPO_7$

formula	$SrCo_2BPO_7$
fw	359.26.
T, K	293(2)
cryst syst	monoclinic
space group	$P2_1/c$
a, Å	6.477(1)
b, Å	9.026(9)
c, Å	10.063(1)
β, deg	111.15(9)
V, Å^3	548.7(2)
Z	4,
D_c, g cm^{-3}	4.349
μ, mm^{-1}	19.403
GOF on F^2	1.1
R1, wR2 [$I > 2\sigma(I)$]^a	0.0290, 0.0661
R1, wR2 (all data)	0.0323, 0.0680

^{a}R1 = $\sum||F_o| - |F_c||/\sum|F_o|$, wR2 = $\{\sum w[(F_o)^2 - (F_c)^2]^2/\sum w[(F_o)^2]^2\}^{1/2}$.

Magnetic Measurements. Magnetic and heat capacity measurements were performed using a commercial Quantum Design Physical Property Measurement System (PPMS). Powdered samples (57 mg) of $SrCo_2BPO_7$ were placed in a gel capsule sample holder which was suspended in a plastic drinking straw. Magnetic susceptibility was measured at 0.1 T from 300 to 2 K (temperature scan of 5 K/min), and magnetization was measured at 2 and 20 K in applied field from −8 to 8 T (field scan of 0.1 T/step). Heat capacity was measured at zero field by a relaxation method using a pellet sample (2.5 × 2.7 mm^2, ~15.4 mg).

RESULTS AND DISCUSSION

Structural Descriptions. $SrCo_2BPO_7$ crystallizes in the monoclinic space group $P2_1/c$ with a = 6.477(1) Å, b = 9.026(9) Å, c = 10.063(1) Å, and β = 111.15(9)°. There are one Sr atom, two Co atoms, one B atom, and one P atom in the asymmetric unit. As shown in Figure 1, B atoms are

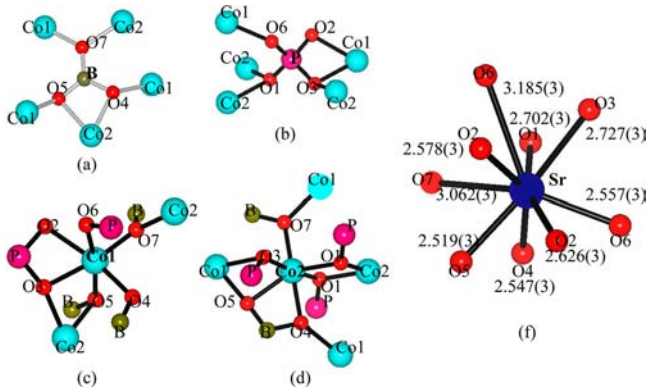

Figure 1. Oxygen-coordination environments for (a) B, (b) P, (c) Co1, (d) Co2, and (f) Sr atoms, respectively.

coordinated by three oxygen atoms, forming a planar BO_3 triangle with B–O bond lengths ranging from 1.367(6) to 1.382(5) Å. P atoms are tetrahedrally coordinated by four oxygen atoms, forming a distorted PO_4 tetrahedron with P–O bond lengths ranging from 1.528(3) to 1.558(3) Å. Both BO_3 triangles and PO_4 tetrahedra are isolated in the titled compound, which are similar to those groups in borophosphate compounds M_3BPO_7 (M = Co, α, β-Zn, Mg).[23,28,29] Cobalt atoms have two independent crystallographic sites (Co1 and Co2), which are coordinated by six oxygen atoms, forming CoO_6 octahedra. All of CoO_6 octahedra are distorted with Co–O bond lengths ranging from 2.002(3) to 2.293(3) Å and O–Co–O bond angles of CoO_6 octahedron ranging from 66.13(11)° to 174.29(14)°. Such distortion of CoO_6 octahedra is due to asymmetric six-oxygen-coordination geometry affected strongly by BO_3 triangles or PO_4 tetrahedra, in which Co1 atoms connect to P atoms by edge-sharing and corner-sharing oxygen atoms, while Co2 atoms are also surrounded by edge-sharing and corner-sharing BO_3 triangles. Oxygen atoms have seven independent crystallographic sites. Besides O2 and O6 sites connected to two atoms (P and Co1) in the framework, other O sites are linked by three atoms (B, Co1, Co2, or P). Strontium atoms are surrounded by nine oxygen atoms with Sr–O bond lengths ranging from 2.519(3) to 3.185(3) Å.

As shown in Figure 2, $SrCo_2BPO_7$ features a complicated three-dimensional (3D) framework, containing warping $[B_2Co_4O_{14}]_\infty$ layers which are composed of four-column $[Co_4O_{18}]$ ribbons and BO_3 triangles. Such warping $[B_2Co_4O_{14}]_\infty$ layers are connected by PO_4 tetrahedra to form the 3D network, in which strontium atoms locate inside the tunnels along [101] direction. As shown in Figure 3, a four-column ribbon $[Co_4O_{18}]$ is built by the edge-sharing CoO_6 octahedra with Co1–Co2–Co2–Co1 manner. This is quite similar to ribbons with the arrangement of M^{2+}–M^{3+}–M^{3+}–M^{2+} in warwickites $M^{2+}M^{3+}OBO_3$.[18] Further, the CoO_6 ribbons connect to each other by corner-sharing oxygen, forming a warping $[Co_4O_{14}]_\infty$ layer, in which the triangle BO_3 located in the voids between the ribbons.

dx.doi.org/10.1021/ic3023979 | Inorg. Chem. 2013, 52, 2492–2496

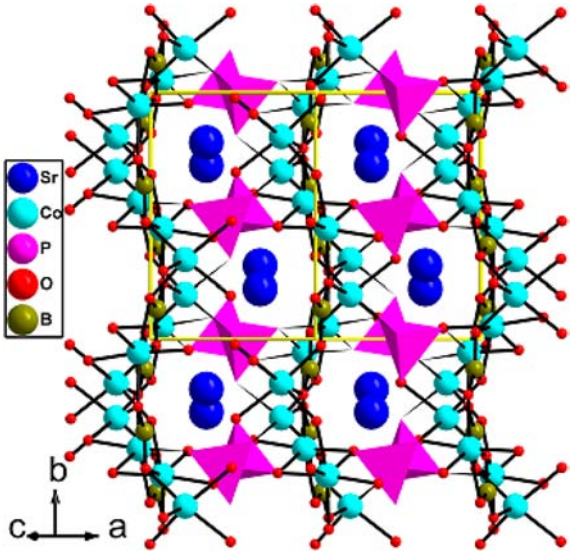

Figure 2. Crystal structure of $SrCo_2BPO_7$ viewing along the [101] direction. The warping layers are seen.

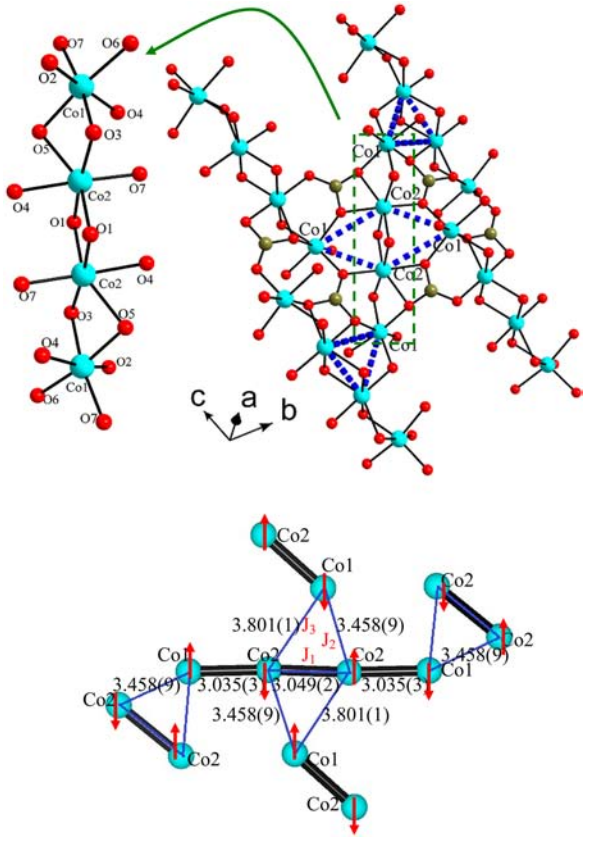

Figure 3. Linkage of four-column ribbons with Co1−Co2−Co2−Co1 manner. Triangles built by Co^{2+} ions (blue dotted lines) are seen between ribbons and the spin arrangements (arrows) of Co^{2+} ions in triangles with different distances (Å) and different exchanges (*J*1, *J*2, and *J*3). The thick lines show the four-column ribbons.

In fact, the four-column $[Co_4O_{18}]$ ribbons in $SrCo_2BPO_7$ are quite skewed due to the linkage of distorted CoO_6 octahedra by edge-sharing. However, to further check the linkage of CoO_6 octahedra, we note that the connection of ribbons is corner-sharing. Thus, there are irregular triangles with different distances of Co2−Co2 [3.049(2) Å], Co1−Co2 [3.801(1) Å], and Co1−Co2 [3.458(9) Å], which are built up by the Co2−Co2 dimers in ribbons and Co1 atoms in the nearest neighboring ribbons as seen in Figure 3.

Magnetic Properties. Figure 4 shows the temperature dependences of the magnetic susceptibility for polycrystalline

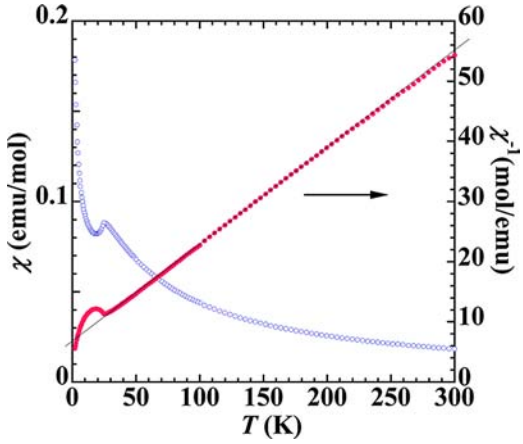

Figure 4. Temperature dependences of the magnetic susceptibility and corresponding reciprocal susceptibility for $SrCo_2BPO_7$.

$SrCo_2BPO_7$. The susceptibility increases with decreasing temperature, while a peak is observed around 25 K, showing the onset of antiferromagnetic ordering. A Curie-like upturn in susceptibility is seen around 5 K, suggesting origination from the contribution of a small amount of paramagnetic impurity such as the isolated Co^{2+} ions due to lattice defect. The concrete evidence for paramagnetic component instead of weak ferromagnetism is seen in the magnetization and heat capacity data (Figures 5 and 6). As seen in the inverse susceptibility, a

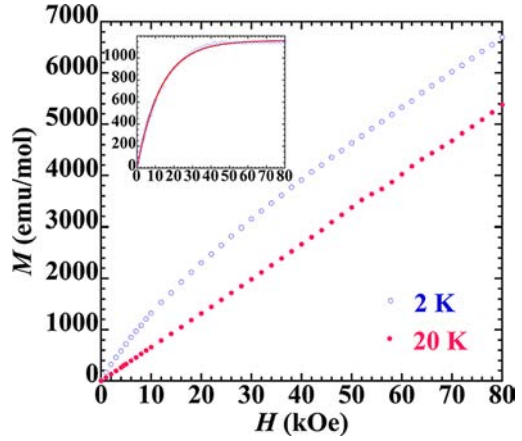

Figure 5. Magnetization as a function of applied field *H* at 2 and 20 K. The inset shows moment arising from paramagnetic impurity at 2 K through subtracting the linear component in the magnetization. The red solid line shows a fit using the Brillouin function with $S = {}^3/_2$.

typical Curie−Weiss behavior is observed above 40 K, giving the Curie constant C = 6.266(3) emu K/mol and Weiss temperature θ = −42.1(2) K. The effective magnetic moment of Co^{2+} ions in the system is calculated to be 5.00(6) μ_B, which is larger than the value 3.873 μ_B obtained by Co^{2+} ($S = {}^3/_2$) ions, indicating a large orbital moment contribution of Co^{2+} in oxygen octahedral environment. Also, the negative Weiss

dx.doi.org/10.1021/ic3023979 | Inorg. Chem. 2013, 52, 2492−2496

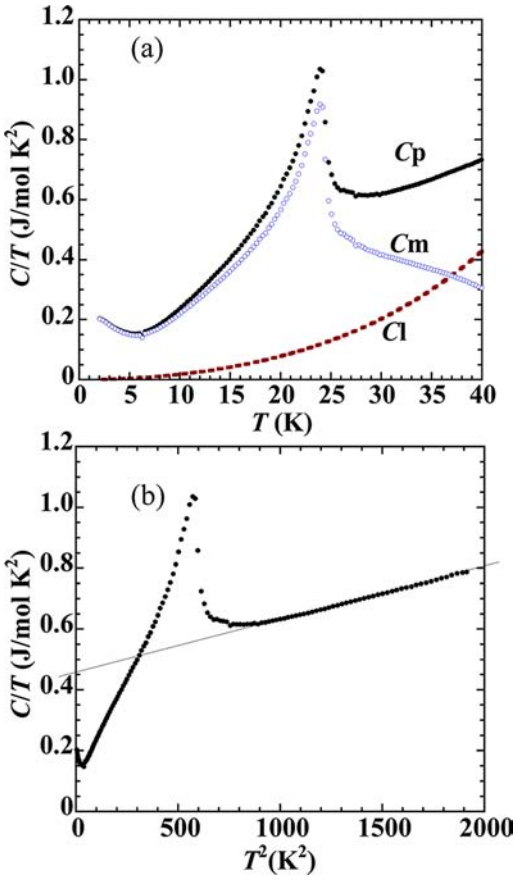

Figure 6. (a) Heat capacity measured in zero magnetic field. The red dashed line represents the lattice contribution (C_l) to heat capacity and blue opened circles are magnetic contribution (C_m). (b) Linear relation of C/T vs T^2 above 33 K.

temperature indicates that the interactions between magnetic Co^{2+} ions are antiferromagnetic in nature.

Figure 5 shows the magnetization as a function of applied field (M–H) at different temperatures. At 2 K, the magnetization rapidly increases in the low field region, while a linear behavior of magnetization is seen at $H > 20$ kOe. The moment arising from paramagnetic impurity (M_{para}) can be obtained by subtracting the linear component ($M_{para} = M - \chi H$) in the magnetization (see the inset of Figure 5). We note the M_{para} versus H curve can be well reproduced by Brillouin function of $S = {}^3/_2$, confirming that the upturn of susceptibility below 5 K is not of a weak ferromagnetic component but is a typical one for paramagnetic impurity. Also, the saturated magnetization of ~0.099 μ_B/Co^{2+} can be obtained for paramagnetic impurity, corresponding to ~3.3% isolated Co^{2+} ions in the system. At 20 K, a linear behavior of magnetization is observed, confirming a collinear antiferromagnetic ordering at ~25 K. Figure 6 shows the results of heat capacity measurements in $H = 0$. There is a sharp peak at ~25 K, giving concrete evidence for a long-range antiferromagnetic ordering at ~25 K. We note that the increases of heat capacity at around 5 K may be a tail of Schottky type heat capacity of paramagnetic impurity. In addition, the heat capacity data above 33 K can be well fitted to $C_p = \gamma T + \beta_1 T^3$ with $\gamma = 0.457(8)$ J mol^{-1} K^{-1} and $\beta_1 = 1.72(2) \times 10^{-4}$ J mol^{-1} K^{-4}. Since $SrCo_2BPO_7$ is an insulator, it is reasonable to arrange the γT term to the magnetic contribution (C_m) and the $\beta_1 T^3$ term to the lattice contribution (C_l). Therefore, the magnetic contribution below 30 K was calculated as $C_m = C_p - C_l$, and the magnetic entropy change for λ-like anomaly around 25 K was roughly estimated to be ΔS = ~3.48 J/(mol K), which corresponds to ~30.2% of $R \ln(2S + 1)$ expected for spin-${}^3/_2$ systems. Also, the Debye temperature of 513.7 K can be estimated by the formula $\beta = 12\pi^4 Rn/(5\Theta_D{}^3)$, where R, n, and Θ_D are the gas constant, the number of atoms per formula unit (in this case $n = 12$), and the Debye temperature, respectively.

The above results combined from magnetic and heat capacity measurements confirmed that the titled material exhibits a long-range antiferromagnetic ordering at ~25 K. We now discuss the possible spin arrangements in $SrCo_2BPO_7$ with a ribbon structure. For many ribbon compounds such as warwickites,[19] it has been pointed out that magnetic behaviors are determined by the intraribbon and interribbon interactions, in which the value of θ_{CW} displays the intraribbon interactions, while the T_N is determined by the interribbon interactions. As shown in inverse susceptibility in Figure 4, the negative Weiss temperature indicates that the intraribbon interactions are antiferromagnetic couplings, so we can presume the spin up–down alignments in a four-column ribbon to be Co1 (↓) Co2 (↑) Co2 (↓) Co1 (↑) or the inverse direction at each site as seen in Figure 3. We note that the irregular triangles between ribbons have three exchange couplings ($J1$, $J2$, and $J3$) with different distances of Co2–Co2 (3.0498 Å), Co1–Co2 (3.4590 Å), and Co1–Co2 (3.8015 Å), respectively. It is well-known that the Hamiltonian for exchange interaction between any two spins (S_1 and S_2) can be expressed as $H = -2JS_1 \cdot S_2$, where the magnitude and the sign of the exchange constant J are determined by the bonding geometry according to the Goodenough rules.[30] Considering different coupling distances between Co^{2+} ions (Figure 3), the antiferromagnetic exchange constants seem to be $J1 > J2 > J3$. As a result, the spins might be arranged well in the nonequilateral triangles between the ribbons as shown in Figure 3, and spin frustration likely does not occur. Actually, the value of $f = 1.68$ ($\theta = -42$ K, $T_N = \sim 25$ K) is obtained for $SrCo_2BPO_7$, based on an empirical measure[31] for spin-frustration proposed by defining the value of $f = |\theta_{CW}|/T_N$, clearly ruling out significant geometrical frustration in the system. This shows that the irregular triangles built by Co^{2+} ions in $SrCo_2BPO_7$ are quite different from geometrically frustrated systems[32] such as Kagome and pyrochlore lattices which the spins in equilateral triangle and tetrahedron cannot simultaneously minimize all the interaction energies.

■ CONCLUSIONS

In summary, a new borophosphate $SrCo_2BPO_7$ has been synthesized by a conventional high-temperature solid-state reaction. The titled compound was found to crystallize in monoclinic system with space group $P2_1/c$, which displays a distorted four-column ribbon [Co_4O_{18}] structure. The irregular triangles built by Co^{2+} ions were found to exist in the connecting ribbons. Susceptibility, magnetization, and heat capacity measurements confirmed that $SrCo_2BPO_7$ possesses an antiferromagnetic at 25 K. We suggest the spin up–down alignments in a four-column ribbon to be Co1 (↓) Co2 (↑) Co2 (↓) Co1 (↑) or the inverse direction at each site.

■ ASSOCIATED CONTENT

Supporting Information

Additional figures and tables. This material is available free of charge via the Internet at http://pubs.acs.org.

dx.doi.org/10.1021/ic3023979 | Inorg. Chem. 2013, 52, 2492–2496

AUTHOR INFORMATION

Corresponding Author

*E-mail: hcz1988@hotmail.com or hezz@fjirsm.ac.cn.

Notes

The authors declare no competing financial interest.

ACKNOWLEDGMENTS

This work was financially supported by the NSFC (Grant 11074250), the National Basic Research Program of China (2012CB921701), the NSF of Fujian Province (2010J01019), and Program for Excellent Talents in Fujian Province.

REFERENCES

(1) Meisel, W.; Guttnann, H. J.; Gütlich, P. *Corros. Sci.* **1983**, *23*, 1373.
(2) Moffat, J. B. *Catal. Rev. Sci. Eng.* **1978**, *18*, 199.
(3) Padhi, A.; Nanjundaswamy, K.; Goodenough, J. *J. Electrochem. Soc.* **1997**, *144*, 1168.
(4) Moqine, A.; Boukhari, A.; Darriet, J. *J. Solid State Chem.* **1993**, *107*, 362.
(5) Belik, A. A.; Azuma, M.; Matsuo, A.; Whangbo, M. H.; Koo, H. J.; Kikuchi, J.; Kaji, T.; Okubo, S.; Ohta, H.; Kindo, K.; Takano, M. *Inorg. Chem.* **2005**, *44*, 6632.
(6) Belik, A. A.; Azuma, M.; Matsuo; Kaji, T.; Okubo, S.; Ohta, H.; Kindo, K.; Takano, M. *Phys. Rev. B* **2006**, *73*, 024429.
(7) Regnault, L. P.; Rossat-Mignod, J.; Henry, J. Y.; Dejongh, L. J. *J. Magn. Magn. Mater.* **1983**, *31*−*34*, 1205.
(8) He, Z.; Chen, S. C.; Lue, C. S.; Cheng, W.-D.; Ueda, Y. *Phys. Rev. B* **2008**, *78*, 212410.
(9) Regnault, L. P.; Rossat-Mignod, J. *Physica B* **1977**, *86*−*88*, 660.
(10) He, Z.; Ueda, Y. *Solid State Commun.* **2008**, *147*, 24.
(11) Belik, A. A.; Azuma, M.; Takano, M.; Lazoryak, B. I. *Chem. Mater.* **2004**, *16*, 4311.
(12) Becker, P. *Z. Kristallogr.* **2001**, *216*, 523.
(13) Becker, P. *Adv. Mater.* **1998**, *10*, 979.
(14) Attfield, J. P.; Bell, A. M. T.; Rodriguez-Martinez, L. M.; Greneche, J. M.; Cernik, R. J.; Clarke, J. F.; Perkins, D. A. *Nature* **1998**, *396*, 655.
(15) Continentino, M. A.; Pedreira, A. M.; Guimaraes, R. B.; Mir, M.; Fernandes, J. C.; Freitas, R. S.; Ghivelder, L. *Phys. Rev. B* **2001**, *64*, 014406.
(16) Goff, R. J.; Williams, A. J.; Attfield, J. P. *Phys. Rev. B* **2004**, *70*, 014426.
(17) Rivas-Murias, B.; Rivadulla, F.; Sanchez-Andujar, M.; Castro-Couceiro, A.; Senaris-Rodriguez, M. A.; Rivas, J. *Chem. Mater.* **2006**, *18*, 4547.
(18) Norrestam, R.; Kritikos, M.; Sjodin, A. *J. Solid State Chem.* **1995**, *114*, 311.
(19) Guimaraes, R. B.; Fernandes, J. C.; Continentino, M. A.; Borges, H. A.; Moura, C. S.; da Cunha, J. B. M.; dos Santos, C. A. *Phys. Rev. B* **1997**, *56*, 292.
(20) Fletcher, J. G.; Glasser, F. P.; Howie, R. A. *Acta Crystallogr., Sect. C* **1991**, *47*, 12.
(21) Zhang, W.-L.; Lin, C.-S.; Geng, L.; Li, Y.-Y.; Zhang, H.; He, Z.-Z.; Cheng, W.-D. *J. Solid State Chem.* **2010**, *183*, 1108.
(22) Meisel, M.; Paech, M.; Wilde, L.; Wulff-Molder, D. *Z. Anorg. Allg. Chem.* **2004**, *630*, 983.
(23) Yilmaz, A.; Bu, X.-H.; Kizilyalli, M.; Kniep, R.; Stucky, G. D. *J. Solid State Chem.* **2001**, *156*, 281.
(24) Bontchev, R. P.; Sevov, S. C. *Inorg. Chem.* **1996**, *35*, 6910.
(25) Zhang, W.-L.; He, Z.-Z.; Xia, T.-L.; Luo, Z.-Z.; Zhang, H.; Lin, C.-S.; Cheng, W.-D. *Inorg. Chem.* **2012**, *51*, 8842.
(26) Sheldrick, G. M. *Crystallographic Software Package, SHELXTL*, version 5.1; Bruker-AXS: Madison, WI, 1998.
(27) Spek, A. L. *J. Appl. Crystallogr.* **2003**, *36*, 7.
(28) Liebertz, J.; Stahr, S. *Z. Kristallogr.* **1982**, *160*, 135.
(29) Wang, G.-F.; Wu, Y.-C.; Fu, P.-Z.; Liang, X.-Y.; Xu, Z.-Y.; Chen, C.-T. *Chem. Mater.* **2002**, *14*, 2044.
(30) Goodenough, J. B. *Phys. Rev.* **1960**, *117*, 1442.
(31) Schiffer, P.; Ramirez, A. P. *Commun. Condens. Matter Phys.* **1996**, *10*, 21.
(32) Greedan, J. E. *J. Mater. Chem.* **2001**, *11*, 37.